PNAS RESEARCH ARTICLE | IMMUNOLOGY AND INFLAMMATION OPEN ACCESS

Antibody reactivity against EBNA1 and GlialCAM differentiates multiple sclerosis patients from healthy controls

Neda Sattarnezhad[a,b,1], Ingrid Kockum[c,d,1], Olivia G. Thomas[c,e], Yicong Liu[c,d], Peggy P. Ho[f], Alison K. Barrett[g], Alexandros I. Comanescu[g], Tilini U. Wijeratne[a], Paul J. Utz[a], Lars Alfredsson[c,h], Lawrence Steinman[f,2], William H. Robinson[a,i], Tomas Olsson[c,d,1,2], and Tobias V. Lanz[a,g,1,2]

Affiliations are included on p. 9.

Contributed by Lawrence Steinman; received December 3, 2024; accepted December 19, 2024; reviewed by Lars Fugger and Jonathan Kipnis

Multiple sclerosis (MS) is an autoimmune demyelinating disorder of the central nervous system (CNS), which is linked to Epstein–Barr virus (EBV) infection, preceding the disease. The molecular mechanisms underlying this connection are only partially understood. We previously described molecular mimicry between the EBV transcription factor EBV nuclear antigen 1 (EBNA1) and three human CNS proteins: anoctamin-2 (ANO2), alpha-B crystallin (CRYAB), and glial cellular adhesion molecule (GlialCAM). Here, we investigated antibody responses against EBNA1 and GlialCAM in a large cohort of 650 MS patients and 661 matched population controls and compared them to responses against CRYAB and ANO2. We confirmed that elevated IgG responses against EBNA1 and all three CNS-mimic antigens associate with increased MS risk. Blocking experiments confirmed the presence of cross-reactive antibodies and molecular mimicry between EBNA1 and GlialCAM, and accompanying antibody responses against adjacent peptide regions of GlialCAM suggest epitope spreading. Antibody responses against EBNA1, GlialCAM, CRYAB, and ANO2 are elevated in MS patients carrying the main risk allele *HLA-DRB1*15:01,* and combinations of *HLA-DRB1*15:01* with anti-EBNA1 and anti-GlialCAM antibodies increase MS risk significantly and in an additive fashion. In addition, antibody reactivities against more than one EBNA1 peptide and more than one CNS-mimic increase the MS risk significantly but modestly. Overall, we show that molecular mimicry between EBNA1 and GlialCAM is likely an important molecular mechanism contributing to MS pathology.

multiple sclerosis | Epstein–Barr virus | antibodies | molecular mimicry | GlialCAM

Significance

Multiple sclerosis (MS) is an autoimmune disease of the brain and spinal cord, leading to disability in young adults. Infection with Epstein–Barr virus (EBV) is a prerequisite for developing the disease. We previously demonstrated that antibody responses against the virus protein EBV nuclear antigen 1 (EBNA1) cross-react with brain proteins of MS patients and contribute to the disease. Here, we confirm in a large cohort of MS patients and controls that the presence of these antibodies increases the risk for MS, and we correlate them with the major genetic risk factor for MS. A combination of multiple antibodies and the genetic risk factor increases the risk for MS in an additive fashion.

Multiple sclerosis (MS) is the most common cause of nontraumatic disability in young adults. It is an autoimmune demyelinating disorder, where aberrantly activated B and T cells from the adaptive arm of the immune system, and macrophages from the innate arm of the immune system, attack the myelin sheaths in the central nervous system (CNS). Demyelination is followed by neuronal loss and widespread activation of the brain's glial cells. While tremendous progress has been made in controlling disease activity and delaying progression of disability, much of the pathophysiology of MS remains to be elucidated (1). The ubiquitous herpesvirus Epstein–Barr virus (EBV) is strongly associated with MS and is considered a prerequisite for developing the disease (2). However, a conundrum arises because only a small percentage of individuals infected with EBV develop MS. Thus, additional genetic and environmental factors are involved before clinical disease appears. In addition to EBV infection, symptomatic infectious mononucleosis (IM) and highly elevated titers of serum antibodies against EBV nuclear antigen 1 (EBNA1) are additional independent risk factors for MS (3, 4). Other risk factors include low vitamin D levels, smoking, and carrying MS risk genes, including the human leukocyte antigen (HLA) class II allele *HLA-DRB1*15:01,* the most significant risk gene for MS. Most of the environmental/lifestyle factors interact with MS HLA risk genes, leading to substantially increased Odds ratios (ORs). Since HLA class II genes regulate CD4+ T cells, the interactions with such genes argue for mechanisms of the environmental factors acting through adaptive immunity, just as MS risk genes (5–7).

On a molecular level, the link between EBV and MS is incompletely understood. Studies found evidence for several mechanisms, including altered anti-EBV T cell responses in MS patients (8–11), unstable EBV latency in infected B cells (12), and dysregulation of genes associated with autoimmunity, largely mediated by the EBV transcription factor EBNA2 (13). We and others described molecular mimicry between the EBV transcription factor EBNA1 and CNS antigens, including anoctamin 2 (ANO2), glial cellular adhesion molecule (GlialCAM), Alpha-B crystallin (CRYAB), and myelin basic protein (MBP) (14–17). The pathogenic relevance of several of these mimics was supported by animal

Competing interest statement: T.O. has received lecture/advisory board honoraria from Biogen, Merck, Novartis and Sanofi, and unrestricted MS research grants from the same companies. W.H.R. and T.V.L. are stockholders and consultants of Ebvio and Flatiron Bio., T.V.L. and W.H.R. filed a patent with Stanford University: US 2024/0309451 A1. L.S. has received lectureship, advisory board honoraria from Roche, Bristol Meyers Squibb, Merck, GSK, and TG Therapeutics relevant to EBV and MS.

[1]N.S., I.K., T.O., and T.V.L. contributed equally to this work.

[2]To whom correspondence may be addressed. Email: steiny@stanford.edu, Tomas.Olsson@ki.se, or tlanz@stanford.edu.

This article contains supporting information online at https://www.pnas.org/lookup/suppl/doi:10.1073/pnas.2424986122/-/DCSupplemental.

Published March 10, 2025.

Table 1. Demographics and clinical characteristics of the study cohort

Characteristic	Case (n = 650)	Control (n = 661)
Age (years), mean (SD)	40.21 (10.32)	42.93 (10.43)
BMI (kg/m^2), mean (SD)	25.06 (4.67)	24.83 (4.32)
Disease duration (years), mean (SD)	4.96 (5.95)	NA
MSSS, median (25th, 75th quartile)	3.65 (1.67, 5.58)	NA
Gender, n (%)		
Male	187 (28.77)	163 (24.66)
Female	463 (71.23)	498 (75.34)
MS course, n (%)		
Control	NA	661 (100)
PPMS	18 (2.77)	NA
PRMS	9 (1.38)	NA
RRMS	536 (82.46)	NA
SPMS	68 (10.46)	NA
NA	19 (2.92)	NA
Infectious mononucleosis, n (%)		
Yes	88 (13.54)	61 (9.23)
No	468 (72.00)	573 (86.69)
Do not know	47 (7.23)	26 (3.93)
NA	47 (7.23)	1 (0.15)
Treatment, n (%)		
None	406 (62.46)	NA
1st line	182 (28.00)	NA
2nd line	30 (4.62)	NA
NA	32 (4.92)	NA

SD, Standard Deviation; BMI, body mass index; MS, multiple sclerosis; PPMS, primary progressive MS; PRMS, progressive relapsing MS; RRMS, relapsing–remitting MS; SPMS, secondary progressive MS; MSSS, multiple sclerosis severity score.

models of MS (14, 15). In most instances, striking sequence homology between EBNA1 and the respective CNS mimic was identified. Interestingly, most mimics are concentrated in a narrow region on EBNA1 between the second glycine-arginine repeat region and the C-terminal DNA binding domain (amino acid residues ~AA380–450). Elevated antibody reactivities against this region are strongly associated with MS (2, 18–21).

Here, we follow up on our initial data that described cross-reactivity between EBNA1 and GlialCAM. We utilized a bead-based assay to screen for IgG reactivity against EBNA1 and GlialCAM in a large cohort that included plasma samples of 650 MS patients and 661 sex- and age-matched population-based controls (Table 1). EBNA1 and GlialCAM proteins were included, as well as individual peptides spanning the regions of interest, and differential levels of reactivities and the individual relationships between reactivities against each region were evaluated. The data corroborate our prior studies in that MS risk is associated with elevated antibody levels against EBNA1 AA386-405 and GlialCAM AA370-389 and the adjacent regions of both proteins. Antibody reactivities against the broader regions of both proteins are strongly associated with each other. Anti-GlialCAM reactivity against the initially described peptide epitope GlialCAM AA370-389 can be blocked with the EBNA1 peptide AA386-405, confirming the presence of cross-reactive antibodies. However, the antibody response against GlialCAM extends beyond this narrow region and encompasses adjacent peptide regions, likely generated by epitope spreading (22, 23).

In addition, we correlate antibody reactivity with allele dose of *HLA-DRB1*15:01*, the strongest MS risk allele. *HLA-DRB1*15:01* conveys a fourfold (heterozygous) and eightfold (homozygous) increased risk for developing MS (6). The allele shapes the adaptive immune response by enabling preferential presentation of certain peptide antigens on antigen-presenting cells (APC). B cells are effective APCs for their cognate antigens and can promote autoreactive CD4 T cell responses. CD4 T cell help, in turn, promotes maturation of B cells and secretion of antibodies. Enhanced binding of myelin antigens and CD4 T cell responses against CNS antigens have been shown (24, 25), and recent data suggest that the *HLA-DRB1*15:01* allele facilitates cross-presentation of intracellular EBV antigens in EBV-infected B cells to be presented on HLA class II (26). HLA-*DRB1*15:01* could be an important factor that facilitates the development of molecular mimicry from an anti-EBNA1 antibody response toward GlialCAM. We show that positive *HLA-DRB1*15:01* status together with elevated antibody reactivity against EBNA1 and either GlialCAM, CRYAB, or ANO2 synergistically increases the risk for MS.

Results

Antibody Reactivity to EBNA1 and GlialCAM Is Associated with Increased MS Risk. Our case–control study included plasma samples from 1,311 individuals, comprising 650 MS cases and 661 age- and sex-matched population-based controls from the Swedish Nationwide Epidemiological Investigation of MS (EIMS) cohort (Table 1) (27). The average age was 40.2 ± 10.32 and 42.9 ± 10.43 y for the MS and control groups, respectively. The female-to-male ratio was 2.47 among cases and 3.05 in the control group, consistent with the gender distribution observed in typical MS cohorts. The majority of MS patients had a relapsing–remitting disease course (82.5%), followed by secondary progressive MS (10.5%), primary progressive MS (PPMS, 2.8%), and progressive relapsing MS (PRMS, 1.4%). IM rates, body mass index (BMI), treatment status, and MS Severity Score are summarized in Table 1. All antibody reactivities in plasma samples were measured using a fluorescence-activated bead-based assay (*SI Appendix*, Table S1). In agreement with prior findings, reactivity to full-length EBNA1 protein was increased in MS patients over controls (OR: 1.97, CI (CI): 1.53 to 2.54) (Fig. 1 and *SI Appendix*, Table S2), and a similar difference was observed for all included truncated EBNA1 protein versions except for the N-terminal glycine/arginine repeat region (EBNA1 GR-repeat, residues AA2-89). The difference was most pronounced for the C-terminal EBNA1 Mimic-Region+DBD (DBD, DNA-binding domain) (OR: 2.67, CI: 2.06 to 3.49, residues AA380-641), which includes the region that resembles GlialCAM, ANO2, CRYAB, and MBP (14–17), and this result was corroborated on a peptide level, as all EBNA1 30mer peptides covering this region (AA361-470) showed differentially elevated antibody reactivities in the MS group, with the most pronounced difference for EBNA1 peptide AA381-410 (OR: 3.27, CI: 2.50 to 4.28). Our data confirmed that elevated antibody levels against the intracellular domain of GlialCAM (GlialCAM ICD, residues AA262-416) were associated with an increased risk for MS (OR: 1.81, CI: 1.40 to 2.34), and the 30mer GlialCAM peptides covering the larger mimic region (AA305-416) were even more strongly associated with MS risk (most strongly associated peptide: GlialCAM AA385-416, OR: 2.63, CI: 2.02 to 3.43). Interestingly, reactivities against the two GlialCAM peptides AA365-394 and AA370-389 were elevated independently of phosphorylation at serine 376. Our initial

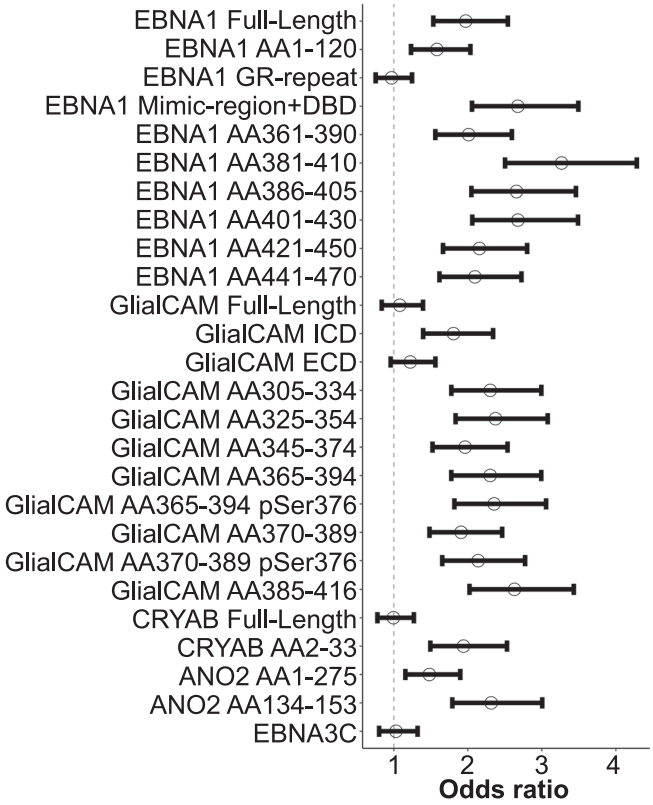

Fig. 1. Individual antibody reactivities associated with MS risk. ORs of MS vs. controls for the indicated antibody reactivities. All data derived from the bead-based assay measuring mean fluorescence intensities. Data were adjusted for age, gender, batch effects, and PCA1-5. ORs were calculated using logistic regression analysis. ORs ±95% CI are shown.

publication had described this posttranslational modification to facilitate molecular mimicry with EBNA1 AA393-398 (14). Consistent with our prior publications, MS risk associated with elevated serum antibody levels against CRYAB AA2-33 (OR: 1.94, CI: 1.49 to 2.53) and ANO2 AA134-153 (OR: 2.32, CI: 1.79 to 3.01) were confirmed (16, 17). The data were adjusted for age, gender, batch effects, and dimensions 1 to 5 of a principal component analysis (PCA) of genetic datasets available for the cohort (28). The threshold for positivity in Fig. 1 was calculated using the median value among controls. For better comparison with prior publications (29, 30), reactivity thresholds were recalculated using the level at which the largest change in MS risk was observed in a sliding window analysis, as well as the largest area under the curve (AUC) metrics, without a significant change in results (*SI Appendix*, Fig. S1). Stratifying MS risk by gender reduces group sizes and subsequently decreases significance levels. There is a trend towards higher ORs in male patients for a few antigens, but overall, gender did not significantly impact the results (*SI Appendix*, Fig. S2).

Overlap between Anti-EBNA1 and Anti-GlialCAM Reactivity. Antibody reactivities against EBNA1 and GlialCAM antigens were compared. Strong correlations of multiple peptides from one antigen support the mechanism of intramolecular epitope spreading, and correlations between EBNA1 and GlialCAM antigens support the mechanism of molecular mimicry between the viral and CNS antigens. Strong correlations were observed among most GlialCAM peptides and EBNA1 peptides, respectively (Fig. 2, *Lower Left* panel and Dataset S1), indicating that isolated reactivity against a single epitope is rare and that intramolecular epitope spreading is a common phenomenon in individuals with antibody responses to GlialCAM. There was a significant overlap between anti-EBNA1 and anti-GlialCAM responses, which included peptides representing the central EBNA1 epitope AA393-398 "SPPRRP," which mimics the central GlialCAM epitope AA377-382 SPPRAP (Fig. 3*A*) (14), but also peptides representing the broader EBNA1 region (AA361-470) and the broader GlialCAM region (AA305-416) (Fig. 2). It supports a close relationship between B cell responses to EBNA1 and GlialCAM, and we hypothesize that once initiated by molecular mimicry, intramolecular epitope spreading increases the breadth of the antibody response. Interestingly, the breadth of the antibody response did not extend to regions far away from the central epitopes, as correlations with anti-EBNA1 AA1-120, anti-EBNA1 GR-repeat (AA2-89), and anti-GlialCAM extracellular domain (ECD) were significantly weaker. Antibody responses against ANO2 AA134-153 overlap with anti-GlialCAM responses more strongly than anti-CRYAB AA2-33 responses (Fig. 2). This is in line with a previously observed divergence of anti-CRYAB and anti-ANO2 responses (16). A notable association was detected between the EBNA1 GR-repeat region, GlialCAM ECD, and the EBV antigen EBNA3C (Fig. 2), three antigens that were not significantly associated with MS risk.

Most of the described correlations were found across the whole cohort and are not unique to MS patients. However, some correlations are more enhanced in MS patients than in controls (Fig. 2, *Top Right* panel). A few correlations of reactivities are worth pointing out, including GlialCAM Full-Length and GlialCAM AA370-389, which associate with several other GlialCAM and EBNA1 antigens more prominently in MS patients than in controls. GlialCAM AA370-389 is prominently correlated with almost all EBNA1 peptides, and also with ANO2 AA1-275, but less so with CRYAB Full-Length (Fig. 2).

Cross-Reactivity between Antibodies against EBNA1 and GlialCAM. Our initial report of molecular mimicry between EBNA1 and GlialCAM described the core epitope regions EBNA1 AA393-398 and GlialCAM AA376-382 (Fig. 3*A*) (14). To determine whether cross-reactive antibodies bind EBNA1 and GlialCAM in this cohort, we subsampled plasma from 10 MS patients with high reactivity to both EBNA1 and GlialCAM and preincubated them with the same antigen, the mimicking antigen, or control peptides before measuring binding. We show that EBNA1 AA386-405 efficiently blocks antibody binding to GlialCAM AA370-389 (Fig. 3 *B* and *F*), confirming the presence of cross-reactive antibodies. In line with our finding that phosphorylation of serine 376 facilitates this molecular mimicry, phosphorylated GlialCAM AA370-389 was more robustly blocked by EBNA1 AA386-405, suggesting stronger molecular mimicry (Fig. 3 *C* and *F*). Interestingly, GlialCAM AA370-389 only partially blocks antibody binding to EBNA1 AA386-405 (Fig. 3 *D* and *F*), which reflects the direction of the development of the B cell response from an initial anti-EBNA1 response toward an anti-GlialCAM response. EBNA1 AA1-120 was used as a negative control peptide (Fig. 3 *E* and *F*).

Impact of *HLA-DRB1*15:01* on Anti-EBNA1 and Anti-GlialCAM Reactivity. *HLA-DRB1*15:01* is the main genetic risk factor for MS and has a major impact on the autoimmune B and T cell response (6, 23–25). To determine whether *HLA-DRB1*15:01* promotes antibody reactivity against GlialCAM in MS patients, we analyzed antibody reactivities against EBNA1 AA381-410 and GlialCAM AA370-389 in groups matched for *HLA-DRB1*15:01* status. Significantly higher IgG levels against both antigens were detected

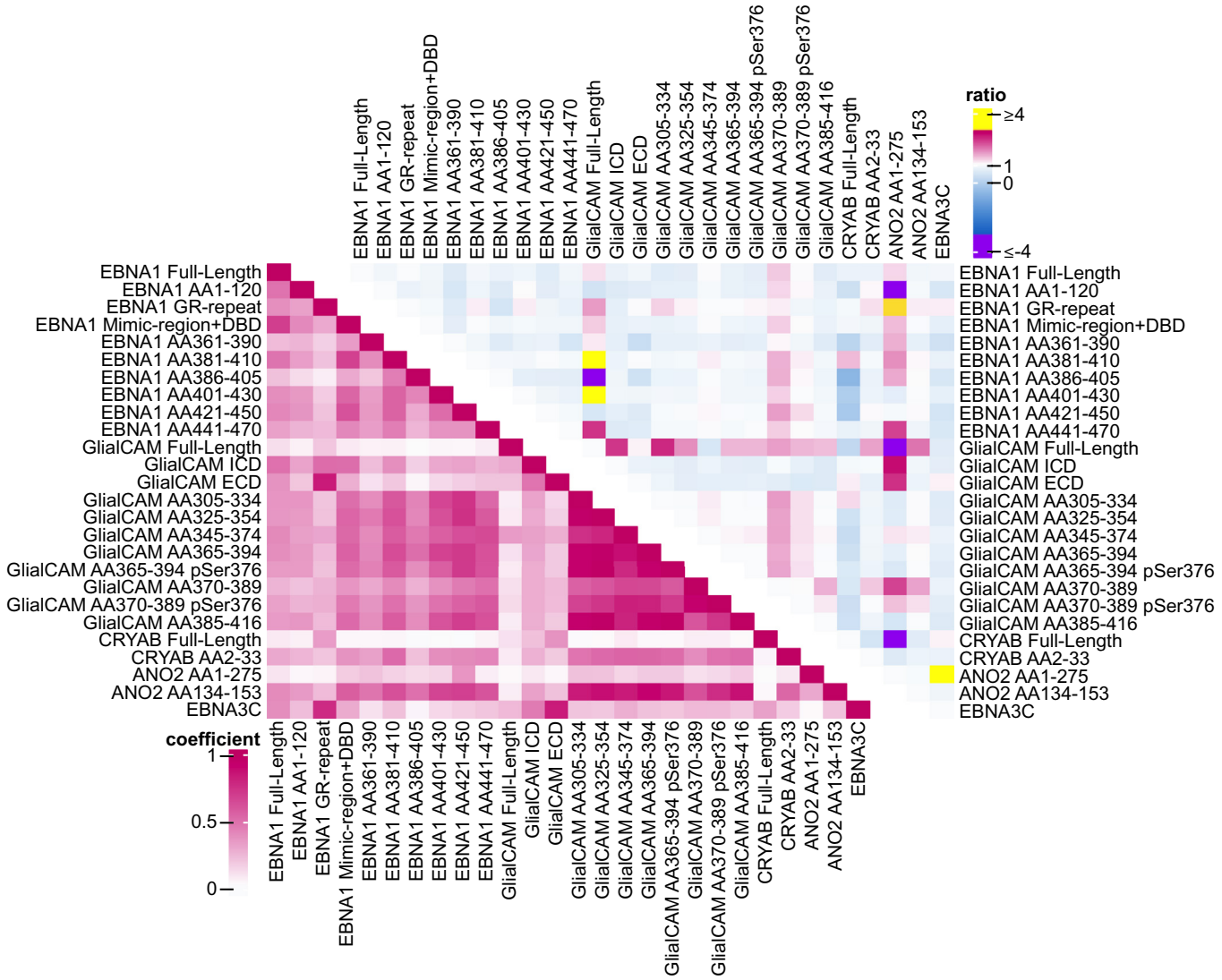

Fig. 2. Correlations of antibody reactivities. (*Lower Left*) Correlation matrix of all tested antigens in all subjects, correlation coefficients of plate-corrected mean fluorescence intensities are shown, calculated using Pearson correlation analysis. (*Top Right*) Matrix showing the ratio of correlation coefficients of the MS vs. control group. Outliers ≥4 (yellow) and ≤-4 (purple) stem from correlation coefficients close to 0 in both groups and do not reflect relevant differences between the two groups.

in MS patients hetero- and homozygous for *HLA-DRB1*15:01*, but the difference was less pronounced in the control group (Fig. 4 *A–F*). Positive *HLA-DRB1*15:01* status and elevated antibody levels against EBNA1 AA381-410 and GlialCAM AA365-394 are three independent risk factors that together increase the MS risk to an OR of 9.40 (CI: 6.04 to 14.86) (Fig. 4*G*). Likewise, there is a cumulative increase in MS risk for *HLA-DRB1*15:01* and anti-EBNA1 AA381-410 in combination with anti-CRYAB AA2-33 (OR: 10.01, CI: 6.38 to 15.97) and *HLA-DRB1*15:01* and anti-EBNA1 AA421-450 anti-ANO2 AA134-153 (OR: 5.42, CI: 3.65 to 8.13) (Fig. 4 *H* and *I*). The protective HLA class I allele *HLA-A*02:01* has the reverse effect, and in combination with elevated antibody levels against EBNA1 AA381-410 and any of the other three antigens, its absence adds additional risk (GlialCAM AA365-394, OR: 19.32 CI: 10.23 to 38.07; CRYAB AA2-33, OR: 17.53, CI: 9.26 to 34.60; ANO2 AA134-153 OR: 11.98, CI: 6.62 to 22.42) (*SI Appendix*, Fig. S3). No significant effect was detected for the additional alleles *HLA-DRB1*03:01*, *HLA-DRB1*08:01*, *HLA-B*38:01*, and *HLA-B*44:02*.

Neurofilament light chain (Nfl) is a marker of neuronal damage that is elevated in EBV-infected MS patients as much as 10 y prior to the onset of MS (2, 31). A correlation between elevated anti-EBNA1 and anti-GlialCAM antibodies might indicate a direct impact of these antibodies on neuronal damage. No significant correlations were observed between antibody reactivity to GlialCAM AA365-394 (r = 0.036, $P = 0.55$) or EBNA1 AA381-410 (r = 0.048, $P = 0.96$) with Nfl levels (*SI Appendix*, Fig. S4).

Cumulative Effects of Multiple Cross-Reactive Antibody Reactivities. A prior study suggested that combinations of multiple antibodies against peptides in the EBNA1 region AA386-445 or antibodies against several of the molecular mimics GlialCAM AA370-389, CRYAB AA2-21, MBP AA205-224, and ANO2 AA135-154 increased the MS risk by 240- to over 1,300-fold (30). We calculated the cumulative risk when combining one or more elevated reactivities against the EBNA1 peptides AA386-405, AA401-430, and AA421-450 and the mimicking peptides GlialCAM AA370-389, CRYAB AA2-33, and ANO2 AA134-153. We determined a significant but moderately elevated cumulative risk over the individual reactivities shown in Fig. 1 with ORs ranging from 2.1 to 3.16 (CI: 1.6 to 2.76 and 2.23 to 4.51, respectively) (Fig. 5).

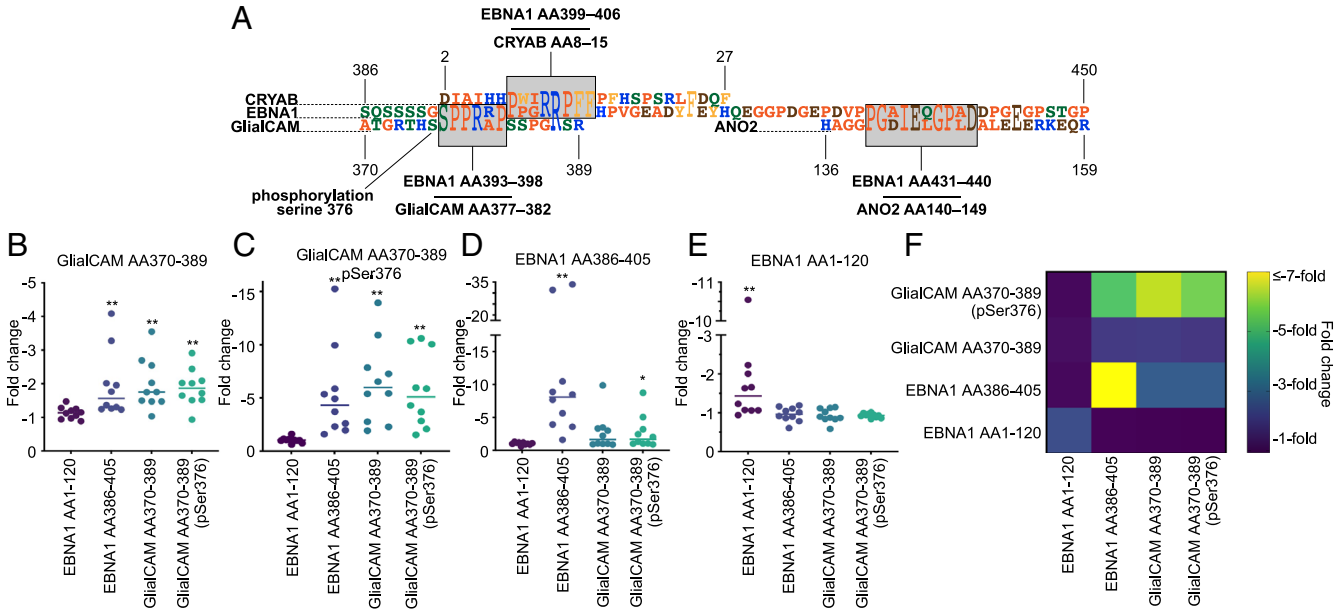

Fig. 3. Cross-blocking of anti-GlialCAM reactivity with EBNA1. (*A*) Alignment of the epitope regions for the molecular mimics GlialCAM, CRYAB, and ANO2 on the EBNA1 sequence. Identical residues span both sequences. Central epitopes are highlighted in gray. Amino acid colors based on side-chain chemistry. (*B–F*) Bead-based competitive blocking assay, measuring reactivity to (*B*) GlialCAM AA370-389, (*C*) GlialCAM AA370-389 pSer376, (*D*) EBNA1 AA386-405, and (*E*) EBNA1 AA1-120 (negative control peptide) after preincubation of selected MS plasma samples (n = 10) with the peptides indicated on the x-axis. Negative fold change of mean fluorescence intensities over samples incubated with BSA indicates increased inhibition. **P* < 0.05, ***P* < 0.005 according to Wilcoxon signed-rank test. (*F*) Heatmap summarizing (*B–E*), showing mean negative fold changes over samples blocked with BSA. *x*-axis: blocking antigen, *y*-axis: bead-based antigen measurement.

Discussion

Increased serum anti-EBNA1 IgG titers are delayed for several weeks to months after an infection with EBV, and their development indicates the end of the acute lytic phase of infection and establishment of viral latency in B cells (32, 33). In most healthy EBV-infected individuals, titers stay elevated for life and MS patients generally have higher anti-EBNA1 IgG titers than healthy individuals (2–4). EBNA1 is a key EBV transcription factor, the only EBV protein that is expressed during all forms of latency (except latency 0), and the only nuclear antigen expressed during the lytic phase of infection (34). In addition to regulating gene expression, it tethers the viral episome to the human chromosome during mitosis and is essential for viral replication and survival during the latent phase. As an immunogen, EBNA1 is unique for several reasons: i) EBNA1 is chronically expressed in B cells at low levels, resulting in repeated antigen exposures over years and decades. This provides the B cell response with ample time to develop from an antiviral response into an autoimmune response through molecular mimicry (2, 31). ii) EBNA1 tightly binds human and viral nucleic acids (35), which likely increases its immunogenicity, akin to several autoantigens that are elevated in rheumatic diseases including systemic lupus erythematosus (SLE) (36). iii) Finally, EBNA1 harbors an immunogenic region between the second glycine-arginine repeat region and the C-terminal DNA binding domain (~AA380–450), with antibodies against this region eliciting molecular mimicry with several CNS antigens in MS as well as lupus antigens in SLE (14–17, 30, 37). Antibody reactivity against this region is higher in MS patients than in healthy EBV-infected individuals (2, 18–21, 30).

Our data confirm prior studies that found elevated anti-EBNA1 antibodies in MS patients (2–4, 19, 38). We found elevated antibody reactivities against full-length protein as well as the truncated domains EBNA1 AA1-120 and EBNA1 Mimic-region+DBD (AA380-641), but not the N-terminal GR-repeat region (AA2-89). As expected, the EBNA1 Mimic-region+DBD yielded the highest relative MS risk of all tested proteins (OR: 2.67, CI: 2.06 to 3.49), superseding EBNA1 Full-Length. An even higher MS risk was observed for the 30mer EBNA1 peptide AA381-410 (OR: 3.27, CI: 2.50 to 4.28), which encompasses the regions that mimic GlialCAM (central epitope: AA393-398) (14) and CRYAB (central epitope: AA399-406, wider epitope: AA399-415) (16) (Fig. 3*A*).

We showed previously that, despite both autoantigens mimicking a common viral protein, MS patients usually have autoantibodies against either CRYAB or ANO2, but less frequently against both antigens (16). This partial exclusion was confirmed here for the regions CRYAB Full-Length and ANO2 AA1-275. We also confirm relatively low autoantibody levels to CRYAB Full-Length, but higher antibody reactivities to linear epitopes of CRYAB and these are associated with MS (16). CRYAB Full-Length tertiary structures seemingly obscure linear epitopes, and a breakdown of CRYAB in inflamed tissues might be necessary for the autoantibody response against CRYAB peptides. Reactivity against all GlialCAM peptides correlated more strongly with ANO2 AA134-153 than with CRYAB AA2-33. In MS patients, GlialCAM ICD and the main GlialCAM epitope AA370-389 correlated strongly with ANO2 AA134-153, but less with CRYAB AA2-33. This might seem counterintuitive, as the mimic regions for GlialCAM and CRYAB on EBNA1 are directly adjacent, whereas ANO2 is located further C-terminal at a distance of approximately 25 amino acids from CRYAB (Fig. 3*A*). A possible explanation for this observation could be steric epitope masking of one EBNA1 epitope by antibodies against the adjacent epitopes during B cell maturation in the germinal center (39). In addition, it is interesting that CRYAB has the properties of an immune checkpoint inhibitor, and an anti-CRYAB response might therefore initiate additional immunomodulatory mechanisms that skew the B cell response, unlike ANO2 and GlialCAM, which share functions as an ion channel

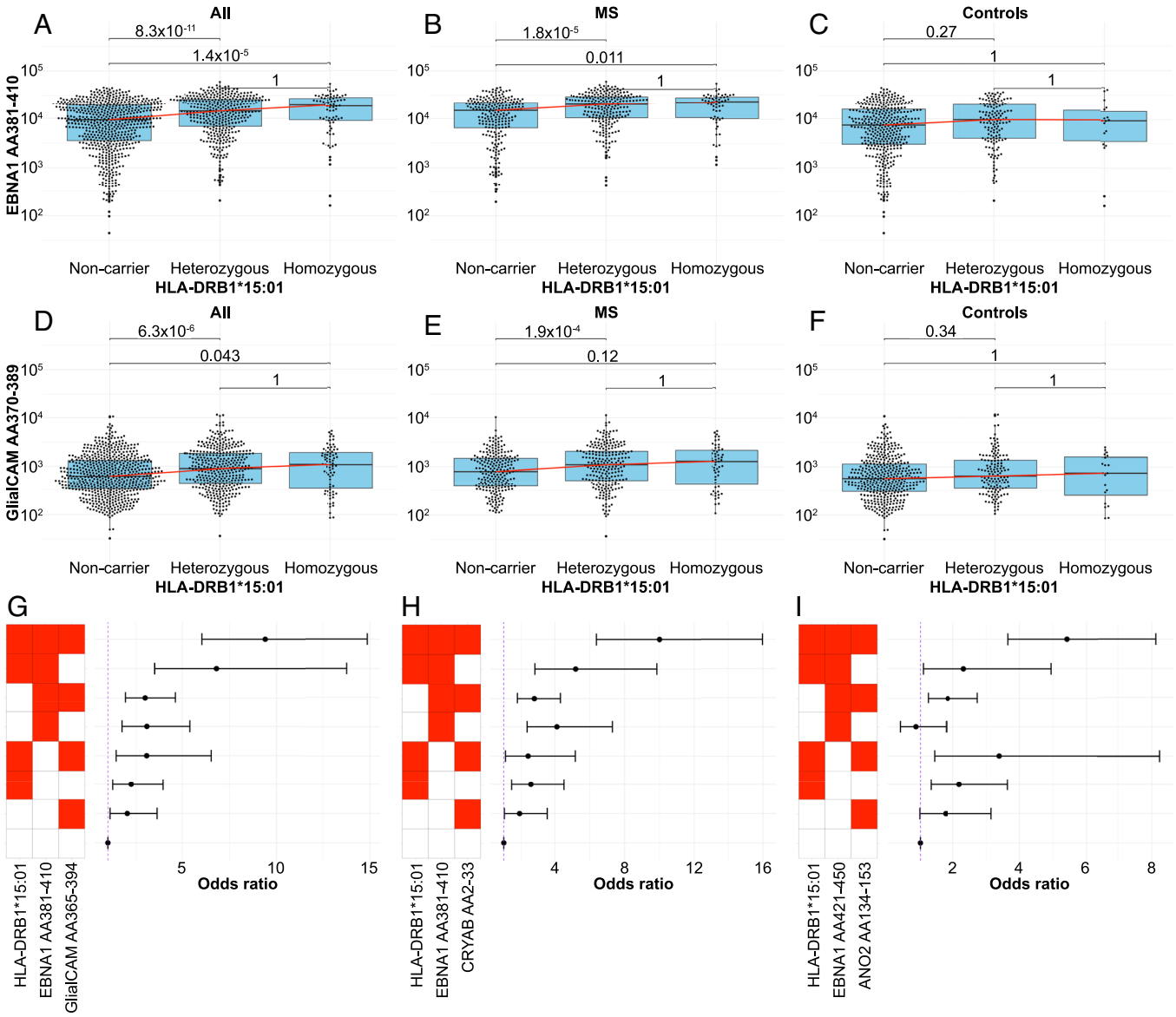

Fig. 4. Association of HLA-DRB1*15:01 status with anti-EBNA1 and anti-GlialCAM antibody reactivity. (*A–C*) Association of *HLA-DRB1*15:01* with anti-EBNA1 AA381–410 reactivity in (*A*) all individuals, (*B*) MS, and (*C*) population controls. (*D–F*) Association of *HLA-DRB1*15:01* with GlialCAM AA370-389 in (*D*) all individuals, (*E*) MS, and (*F*) healthy controls. Indicated *P* values according to the Kruskal–Wallis test. (*G–I*) Plots representing ORs for MS risk for combinations of multiple parameters, including in column 1: positive *HLA-DRB1*15:01* status, in column 2: elevated (*G* and *H*) anti-EBNA1 AA381-410 and (*I*) anti-EBNA1 AA421-450 reactivity, and in column 3: (*G*) anti-GlialCAM AA365-394, (*H*) anti-CRYAB AA2-33, and (*G*) anti-ANO2 AA134-153. Data were adjusted for age, gender, plate-based batch effects, and PCA 1-5. ORs were calculated using logistic regression analysis with the group not having any increased antibody level or being *HLA*DRB15:01* positive (lowest group in each panel) as a reference. ORs ±95% CI are shown.

and an auxiliary subunit of a of an ion channel (CLCN2), respectively (14, 16, 17, 40, 41).

Anti-GlialCAM antibody reactivity is not restricted to the peptide region AA370-389 but was observed for all adjacent peptides ranging from AA305 to AA416, and antibody reactivities against these regions were highly correlated. We demonstrate that reactivity against GlialCAM AA370-389 can be blocked effectively by EBNA1 AA386-405, indicating that the anti-GlialCAM response is spawned from an anti-EBNA1 response. Antibodies against the adjacent regions are likely a result of intramolecular epitope spreading.

While plasma incubation with EBNA1 AA386-405 robustly blocked antibody binding to GlialCAM AA370-389, the inverse experiment showed only partial inhibition, aligning with our understanding of directionality in the development of the anti-GlialCAM antibody response, i.e., stemming from an initial anti-EBNA1 response. This result also indicates an abundance of anti-EBNA1 AA386-405 antibodies, of which only a fraction cross-bind to GlialCAM AA370-389. In contrast, the majority of anti-GlialCAM AA370-389 seemingly develops from the response against EBNA1 AA386-405 and can therefore be cross-blocked. A similar level of directionality was previously observed for ANO2 (17).

Interestingly, antibody responses against GlialCAM ECD did not correlate with responses against the peptides mentioned above spanning the intracellular domain, but rather with a response against the N-terminal GR-repeat region of EBNA1 and EBNA3C. EBNA3C is recognized as an important CD8 T cell antigen (42), but to our knowledge not as a relevant molecular mimic. However, the antigens GlialCAM ECD, EBNA1 GR-repeat region, and EBNA3C individually are not associated with increased MS risk, diminishing the likelihood for their pathological relevance in MS.

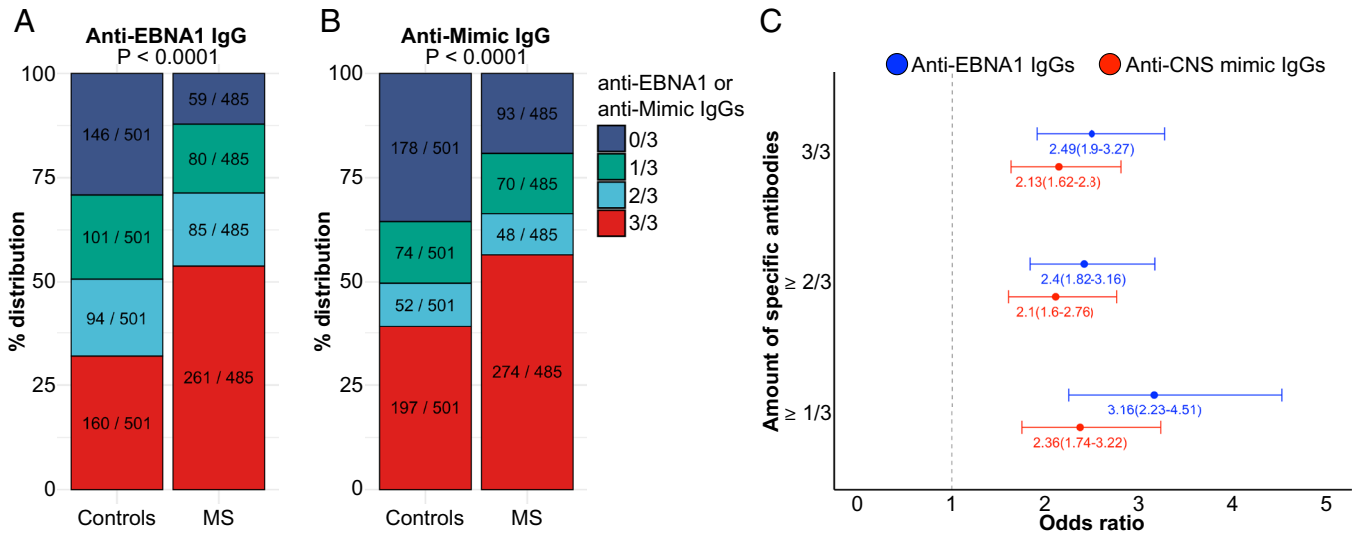

Fig. 5. Cumulative MS risk with multiple combined antibody reactivities against EBNA1 and its three mimics. (*A* and *B*) Distribution of individuals with 0 to 3 elevated antibody reactivities to (*A*) three different EBNA1 peptides (EBNA1 AA386–405, EBNA1 AA401-430, and EBNA1 AA421–450) (*Left*) and (*B*) three different CNS-specific antigens (GlialCAM AA370-389, CRYAB AA2-33, and ANO2 AA134-153) (*Right*). Comparisons between healthy controls and MS are shown. *P* values according to the Chi-square test. (*C*) OR showing cumulative effects of 1 to 3 antibody reactivities. Data were adjusted for age, gender, batch effects, and PCA1-5. ORs were calculated using logistic regression analysis. ORs ±95% CI are shown.

Our initial study on molecular mimicry between EBNA1 and GlialCAM in MS demonstrated that phosphorylation of the serine residue 376 in the GlialCAM protein facilitates cross-binding between the two epitopes (14). Our current data, derived from a significantly larger patient cohort, shows similarly elevated antibody responses against the phosphorylated and unphosphorylated versions of the 30mer GlialCAM AA365-394 and the 20mer GlialCAM AA370-389, and reactivities against the phosphorylated and unphosphorylated versions strongly correlate with each other. The magnitude of blocking by EBNA1 AA386-405, however, was significantly larger for the phosphorylated version of GlialCAM, indicating that this posttranslational modification indeed facilitates molecular mimicry—albeit this might not be essential for the mechanism, or might quickly be overcome by epitope spreading to the nonphosphorylated peptide.

Neuroaxonal damage, indicated by elevated Nfl levels, was reported in preclinical MS approximately a decade after primary EBV infection with or without clinical IM (2, 31). Elevated Nfl levels coincide with the emergence of antibodies against latent and lytic EBV antigens and in some patients with reactivity to ANO2 (31). Association of elevated Nfl levels with antibody reactivity to GlialCAM would suggest a direct impact of anti-GlialCAM antibodies on demyelination and neurodegeneration. Animal studies by us and others indicated that immunization with EBNA1 peptides (AA386-405 and AA411-426) aggravated mouse models of MS and these effects were attributed to increased anti-GlialCAM and anti-MBP B cell responses (14, 15). However, we did not find a correlation with Nfl in our current dataset, indicating that anti-GlialCAM antibodies did not drive neuronal damage at the time of the blood draws of our cohort. At that time, however, all MS patients had been diagnosed with MS, and it would be interesting to determine whether anti-GlialCAM antibodies have a measurable impact on Nfl levels in pre-MS patients or very early postdiagnosis (31).

*HLA-DRB1*15:01* is the major genetic risk factor for MS (6). Preferred presentation of myelin peptides by APCs and activation of CD4 T cells is a likely mechanistic explanation for its pathological relevance in the disease. Multiple studies found the epitope AA83-99 of MBP to be a relevant epitope presented on *HLA-DRB1*15:01* (43, 44). Additionally, there is evidence that humanized *HLA-DRB1*15:01*-positive mice have diminished immune control of EBV despite increased numbers of CD8+ T cells, indicating insufficient CD4+ T cell help to CD8+ T cells (25). In the same mouse model, CD4+ T cell responses against several myelin proteins were induced by EBV infection. Prior studies have found that antibody responses against EBNA1 were elevated in individuals carrying *HLA-DRB1*15:01*, and this included EBNA1 Full-Length protein and fragments spanning the mimicking region AA380-450 (e.g., AA325-641, AA385-420, and AA393-412) (16, 38, 45, 46). Similarly, antibody reactivity against CRYAB AA3-17 was associated with *HLA-DRB1*15:01* (16).

Our study confirms elevated anti-EBNA1 AA381–410 reactivity in MS patients heterozygous and homozygous for *HLA-DRB1*15:01*, and in addition, we show that anti-GlialCAM AA370-389 reactivity is similarly correlated with *HLA-DRB1*15:01* status. Both relationships are more significant in MS patients than in controls, suggesting that *HLA-DRB1*15:01* promotes the development of molecular mimicry between EBNA1 and GlialCAM, and that this mechanism is relevant in MS. We also demonstrate an additive increase of MS risk with i) positive *HLA-DRB1*15:01* status, ii) anti-EBNA1 peptide reactivity, and iii) the corresponding reactivity against the CNS-mimicking peptide, and this is the case for each of the three EBNA1 mimics (*HLA-DRB1*15:01*+EBNA1 AA381-410+GlialCAM AA365-394, OR: 9.40, CI 6.04 to 14.86; *HLA-DRB1*15:01*+EBNA1 AA381-410+CRYAB AA2-33, OR: 10.01, CI 6.38 to 15.97; *HLA-DRB1*15:01*+EBNA1 AA421-450+ANO2 AA134-153, OR: 5.42, CI 3.65 to 8.13). Notably, the absence of the protective HLA class I allele *HLA-A*02:01* is another additive factor that increases the MS risk by a factor of approximately two.

Notably, a prior study had described highly significant differences in anti-GlialCAM AA370-389 IgG levels between MS patients and healthy controls in a cohort of 540 individuals, with *P*-values below 0.0001 (29). 100% of MS patients in this study had relatively high anti-GlialCAM antibody levels, and these were distinct from 60% of healthy controls whose antibody reactivities were approximately twofold lower. Interestingly, anti-GlialCAM AA370-389 antibody reactivity in this study was not associated with *HLA-DRB1*15:01* (29). This clear distinction of all MS

patients from the majority of healthy individuals is different from the data presented here. While we also describe significantly elevated antibody responses against GlialCAM, the significance level is lower, and there is a sizeable number of MS patients in our cohort who do not have elevated anti-GlialCAM antibodies. However, as pointed out above, anti-GlialCAM reactivity is significantly correlated with *HLA-DRB1*15:01*. A follow-up study by the same authors suggested that the combination of multiple highly elevated antibody reactivities against four EBNA1 peptides spanning the region AA386-445 is highly associated with increased MS risk. Similarly, combined elevated antibody reactivities against the three mimicking CNS peptides GlialCAM AA370-389, CRYAB AA2-21, and ANO2 AA135-154, as well as the MBP region AA205-224, are highly associated with MS (30). In this study, over 98% of MS patients had three or more antibody reactivities against either set of peptides, while in healthy individuals either combination was only found in 11.5% and 21.5% of subjects, respectively. The difference between groups that we derived from our data—analyzed in a similar way—reaches significance as well, but it is distinctly smaller: 53.8% of MS patients vs. 31.9% of controls have ≥3 antibodies against EBNA1 peptides, and 56.5% of MS patients vs. 39.3% of controls have ≥3 mimic peptides. The prior study calculated an OR of 655.8 for MS vs. healthy with ≥2 elevated anti-EBNA antibodies and an OR of 1,366 with ≥3 antibodies; with ≥2 antimimic antibodies, the OR was 459.8, and with ≥3 antibodies, it was 243.1. These are impressive numbers that would make tests for these combinations of antibodies valuable supportive biomarkers for MS diagnosis and could even be considered as early detection parameter for at-risk family members of MS patients. Our study, however, does not replicate the increased MS risk associated with these antibodies at the same magnitude. In our cohort, the OR (MS vs. healthy) with ≥1 elevated anti-EBNA antibodies is elevated at 3.16 (CI: 2.23 to 4.51), with ≥2 antibodies at 2.41 (CI: 1.82 to 3.16), and with ≥3 at 2.49 (CI: 1.9 to 3.27). With ≥1 anti-CNS-mimic antibody the OR is 2.36 (CI: 1.74 to 3.22), with ≥2 antibodies it is 2.1 (CI:1.6 to 2.76), and with ≥3 it is 2.13 (CI: 1.62 to 2.8). While significant, our numbers are more than two orders of magnitude lower than those previously described (30). Potential reasons for the observed discrepancy include differences in patient and control cohorts, e.g., the rates of IM were different. However, we tested adjusting our data for IM history and it did not significantly alter our results. In addition, differences could stem from the peptides antigens used: EBNA1 AA386-405 and GlialCAM AA370-389 were used in both studies; EBNA1 AA393-412, EBNA1 AA409-428, CRYAB AA2-21, and ANO2 AA135-154 were used in the prior study (30), whereas EBNA1 AA401-430, EBNA1 AA421-450, CRYAB AA2-33, and ANO2 AA134-153 were used by us; EBNA1 AA426-445 and MBP AA205-224 were not included in our study. Different IgG detection methods were used (ELISA vs. bead-based method), and differences in statistical analyses could have influenced the results to some degree. Our analysis was adjusted for population stratification, sex, age, and plate-based batch effects. However, repeating our analysis adjusting only for sex and age as done previously (30), generated similar results to those in Fig. 5 (*SI Appendix*, Fig. S5). Additional validation studies in large independent cohorts will be necessary to determine the magnitude of increased MS risk levels associated with multiple elevated anti-EBNA1 and antimimic antibodies and their potential usefulness as biomarkers.

In summary, our study demonstrates in a large cohort of MS patients and matched population-based controls that elevated anti-EBNA1 and anti-GlialCAM antibody levels are associated with increased risk for MS. Both elevated reactivities are associated with *HLA-DRB1*15:01,* and a combination of positive *HLA-DRB1*15:01* status, anti-EBNA1 peptide reactivity, and the matching anti-GlialCAM reactivity further increases MS risk in an additive fashion. The same combination with anti-ANO2 and anti-CRYAB reactivities also increases MS risk. While our data are significant, the overall ORs are modest and range from an OR of 3.27 (EBNA1 AA381-410) and an OR of 2.63 (GlialCAM AA385-416) to an OR of 9.40 (combination of *HLA-DRB1*15:01,* anti-EBNA1 AA381-410, anti-GlialCAM AA365-394). Significantly more MS patients harbor between 1 and 3 anti-EBNA1 peptide antibodies and antimimic antibodies than controls, but with ORs between 2.1 and 3.16, the increase in MS risk conveyed by multiple reactivities is also modest. Blocking experiments confirmed cross-reactive antibodies and molecular mimicry between EBNA1 and GlialCAM, and antibody reactivities against multiple intracellular peptides suggest that intramolecular epitope spreading broadens the immune response. Molecular mimicry between EBNA1 and ANO2, CRYAB, and GlialCAM is likely an important molecular mechanism contributing to MS pathology.

Materials and Methods

Patient Cohort. Plasma samples were collected from participants in the Swedish Nationwide EIMS cohort (27). The study included 650 MS patients and 661 population-based controls, matched to MS cases by sex, age, and geographic region. All participants provided written informed consent for sample collection and data analysis. Cohort characteristics are detailed in Table 1. HLA data were previously obtained from studies conducted at the Karolinska Institute (17). Information on IM history and BMI was self-reported via a questionnaire administered at the time of consent and sampling (21, 27, 45). Plasma Nfl levels were quantified using the Single Molecule Array (Simoa™) NF-Light Advantage Kit and normalized for age, sex, and BMI, employing reference data from 1,026 Swedish controls (47). Ethical approval for the study was granted by the Stockholm Ethics Board and Swedish Ethical Review Authority, respectively (no. 04-252/1-4 and no. 2009/2107-3112).

Antigen Selection. Protein and peptide antigens were selected based on prior studies by us and others (9, 14, 48, 49). We focused on the EBV transcription factor EBNA1 and its molecular mimics, which include GlialCAM, CRYAB, and ANO2. Other EBV antigens included in the array are listed in *SI Appendix*, Table S1. Several antigens were represented in multiple versions, including full-length proteins, protein fragments, and peptides. The final array consisted of 26 antigens including 11 GlialCAM, 10 EBNA1, one EBNA3C, two CRYAB full-length and CRYAB AA2-33, and two ANO2 AA1-275 and ANO2 AA134-153.

Protein Expression. EBNA1 was included as full-length protein (AA1-641), two N-terminal regions (AA2-89 and AA1-120), and the C-terminal DBD (AA380-641). GlialCAM was represented by its full-length form (AA34-416), as well as intracellular (AA262-416) and ECD fragments (AA34-240). EBNA1 AA1-641 and AA2-89, and the ECD of GlialCAM (ECD, AA34-240), were expressed in Freestyle 293-F cells (Thermo Fisher Scientific R79007) using second-generation lentiviral transduction. Briefly, constructs were cloned into a custom lentiviral vector (50) and cotransfected into HEK293T cells with second-generation lentiviral packaging plasmids pMD2.G and psPAX2 (Addgene 12259, 12260), and FuGENE (Promega E2312). Lentivirus in supernatants was harvested 72 h posttransfection and used to transduce Freestyle 293-F cells with Polybrene (EMD Millipore TR-1003-G). Cells were cultured to a density of 3 × 10^6 cells/mL, lysed via sonication, and his-tagged proteins were purified with Ni-INDIGO resin (Cube Biotech 75103), followed by size-exclusion chromatography on a Superdex 75 Increase 10/300 GL column (Cytiva 29148721). The N-terminally His-tagged intracellular domain of GlialCAM (AA262-416) was expressed in *Escherichia coli* as previously described (14). EBNA1 (AA1-120), EBNA1 (AA380-641) ANO2 (AA1-275), and CRYAB (full-length) proteins were produced as previously described (16, 51). Briefly, genes were ordered from Eurofins (Luxembourg) and subcloned into a modified vector containing an 8xHis tag. The plasmid was then transformed into BL21-A1 *E. coli*

(Thermo Fisher Scientific C607003) and grown in Vegetone SB medium supplemented with carbenicillin 100 mg/L, 1 mM MgSO4, and 0.6% glycerol for 3 h, before transferring to autoinduction medium (Vegetone SB medium), supplemented with 1 mM $MgSO_4$, 0.6% glycerol, carbenicillin (100 mg/L), 0.015% glucose, 0.2% arabinose, and 0.2% lactose, and incubated overnight at 25 °C. The following day, bacterial pellets were centrifuged at 7,000×g for 30 min and lysed using 6 M Gua-Cl buffer and a freeze–thaw cycle. Lysates were then centrifuged at 20,000×g for 1 h and protein was purified from supernatants using HisMag Sepharose beads (Cytiva 29104065). Sodium dodecyl sulfate–polyacrylamide gel electrophoresis was used to check protein purity and concentrations were determined by NanoDrop (Thermo Fisher Scientific).

Peptide Synthesis. For more granular epitope mapping of selected regions, 30-mer peptides with 10-amino acid overlaps were designed (*SI Appendix*, Table S1) and biotinylated with an amino hexanoic acid spacer (Biomatik, Kitchener, ON, Canada). For EBNA1, 30-mers covered the region AA361–470 with five peptides, and in addition, the 20-mer AA386–405 was included from our previous work (14). For GlialCAM, 30-mer peptides spanned the region AA305–416, with AA365–394 and AA370–389 included in both nonphosphorylated and phosphorylated versions (at serine 376). The CRYAB AA2–33 and ANO2 AA134–153 peptides were included, based on their immunogenic potential in previous studies (16, 17, 38).

Array Preparation. Recombinant proteins were coupled to barcoded carboxylated magnetic beads (MagPlex-C, Luminex Corp.), while biotinylated peptides were coupled to streptavidin-coated magnetic beads (MagPlex-Avidin, Luminex Corp.). For both carboxylated and streptavidin bead coupling, 8 μg of each antigen was coupled to 1×10^6 magnetic beads per bead ID. Beads were washed with an automated Biotek plate washer in 96-well plates (Greiner Bio-One 650201).

Carboxylated beads were washed, resuspended in activation phosphate buffer (0.1 M NaH_2PO_4 pH 6.2; Sigma-Aldrich; S3139-250G), and then incubated with 0.5 mg/mL 1-ethyl-3-(3-dimethylaminopropyl) carbodiimide (Thermo Scientific 77149) and 0.5 mg/mL N-hydroxysuccinimide (Thermo Scientific Pierce 24510) in phosphate buffer for 20 min at room temperature (RT) while shaking in the dark. After washing, beads were resuspended with antigens diluted in coupling buffer [50 mM 2-(N-morpholino)ethanesulfonic acid, pH 5.0; Sigma-Aldrich M2933] and incubated for 120 min at RT while shaking in the dark. Coupled beads were washed twice and then stored in PBS-TBN buffer [phosphate-buffered saline (PBS), 0.1% bovine serum albumin (BSA), 0.02% Tween 20] at 4 °C in the dark until use.

Streptavidin beads were washed, resuspended in antigen solution diluted in PBS+1%BSA (Sigma-Aldrich A8412), and incubated at RT for 30 min while shaking in the dark. Beads were then washed twice with PBS-TBN, resuspended, and stored at 4 °C in the dark until use.

Coupling efficacy was validated using human plasma with known reactivity to EBNA1, GlialCAM, ANO2, and CRYAB, along with monoclonal antibodies against EBNA1 and GlialCAM (14). Bead counts for each bead region were adjusted to ensure uniform counts in the multiplex array.

Array Probing. Plasma samples from MS patients and healthy controls were diluted 1:100 in PBS+1% BSA (Sigma-Aldrich) and 45 μL/well was used in 384-well plates, mixed with 5 μL of bead suspension, and incubated at RT for 60 min in the dark while shaking. After washing, beads were resuspended with secondary antibodies (1:1,000 diluted goat anti-human IgG; Jackson ImmunoResearch 109-117-008) and incubated for 30 min in the dark while shaking. Beads were then washed, resuspended in 50 μL of PBST, and read on the FlexMap 3D system (Luminex Corp.). Results were reported in median fluorescent intensity (MFI), with background MFI values subtracted. Samples with coefficients of variation (CV%) over 40% were reassayed. Researchers were blinded with regard to control vs. patient samples.

Batch Control. MFI of batch control samples (n = 12/plate) was used to normalize average MFI between plates. Samples that after reassay still had high CV (over 30%) were removed. A reference plate was selected for each antigen based on the degree of variability of MFI values on each plate. MFI values of batch control samples in the reference plate with the lowest variability were log-transformed, considering the uncertainty of linear and nonlinear relationships between MFI values in different plates for each antigen. Pearson correlation tests were performed to estimate the possible linear association between MFI values of batch control samples in the reference plate and other plates. Coefficients between the reference plate and other plates were generated for each antigen by linear regression with an intercept as 0. Batch correction was achieved by using a log-transformed average MFI value multiplied with the coefficient of batch control samples in various plates, which was then exponentiated.

EBNA1/GlialCAM Blocking. To confirm cross-reactivity between EBNA1 and GlialCAM, blocking competition assays were conducted. Plasma from 10 selected MS patients (n = 10) was preincubated with EBNA1 AA386–405, GlialCAM AA370–389 (with highest homology to EBNA1 AA386–405), GlialCAM AA370–389-PhosSerine376 (increased antibody binding of GlialCAM with Serine 376 phosphorylation) (14), EBNA1 AA1–120 (a nonhomologous EBNA1 region), or BSA (control) in 0.1 mg/mL of the respective antigen in PBS+1% BSA, for 1 h. Following the preincubation period, signal intensity was probed and analyzed as described in the previous section. Results were evaluated as the fold change in MFI compared to control MFIs (Fig. 3).

Statistical Analysis. Correlations were tested with Pearson correlation tests for continuous variables and Spearman correlation tests for testing monotonic relationships. For continuous variables, *t* tests were used for two-group comparisons, and ANOVA was used for multiple comparisons. Kruskal–Wallis and Dunn's multiple comparison tests were used when normal distribution and homogeneity of variation were violated. Median among controls was used as a cutoff to define individuals with high antibody levels, but as a sensitivity analysis, we used two other cutoffs: the level with the highest change in risk and the level with the highest AUC. Chi-square tests were performed for categorical variables. Linear and logistic regressions were conducted for adjusted comparisons, coefficients, and OR estimation. All statistical analyses were performed in R. Additional details in statistical analysis are available in supplementary materials.

Data, Materials, and Software Availability. Supporting data are included under supporting information. Raw data used to support this study can be accessed as shown (52). As the data is considered to be personal sensitive data access will be granted to any qualified researcher upon request after completing a data access agreement.

ACKNOWLEDGMENTS. This work was supported by grants from the Swedish Research Council (2020-01638), the Swedish Brain Foundation and Horizon Europe (WISDOM project Grant No. 101137154) to I.K.; The Swedish Research Council, The Knut and Alice Wallenberg Foundation, the Swedish Brain Foundation and Knut and Alice Wallenberg Foundation, and Margaretha af Ugglas Foundation to T.O.; the NIH (R01 AI173189) and the US Army Medical Research Acquisition Activity (HT9425-23-1-0595) to W.H.R. and T.V.L.; the Gunvor and Josef Anérs Foundation, NEURO Stockholm, MS Forskningsfonden and NEURO Sweden to O.G.T., the Stanford School of Medicine Dean's Postdoctoral Fellowship to A.K.B., and the NIH (5T32AR050942-18) and National Institute of Allergy and Infectious Diseases (1K23AI177932-01A1) to N.S. L.S. has received support for the John Endriz Fund, the Phil N Allen Trust, and the Zimmermann Endowed Professorship.

Author affiliations: [a]Division of Immunology and Rheumatology, Department of Medicine, Stanford University School of Medicine, Stanford, CA 94305; [b]Department of Neurology, Veterans Affairs Palo Alto Health Care System, Palo Alto, CA 94304; [c]Neuroimmunology Unit, Department of Clinical Neuroscience, Karolinska Institutet, Stockholm 171 76, Sweden; [d]Center for Molecular Medicine, Karolinska University Hospital, Stockholm 171 76, Sweden; [e]Department of Clinical Neuroscience, Therapeutic Immune Design, Center for Molecular Medicine, Karolinska Institute, Stockholm 171 77, Sweden; [f]Department of Neurology and Neurological Sciences, Beckman Center for Molecular Medicine, Stanford University School of Medicine, Stanford, CA 94305; [g]Institute for Immunity, Transplantation, and Infection, Department of Medicine, Stanford University School of Medicine, Stanford, CA 94305; [h]Unit of Occupational Medicine, Institute of Environmental Medicine, Karolinska Institutet, Stockholm 171 77, Sweden; and [i]The Geriatric Research, Education, and Clinical Center, Veterans Affairs Palo Alto Health Care System, Palo Alto, CA 94304

Author contributions: N.S., I.K., O.G.T., P.P.H., L.S., W.H.R., T.O., and T.V.L. designed research; N.S., I.K., O.G.T., Y.L., P.P.H., A.K.B., A.I.C., T.U.W., and T.V.L. performed research; I.K., P.J.U., L.A., L.S., W.H.R., and T.O. contributed new reagents/analytic tools; N.S., I.K., O.G.T., Y.L., L.S., W.H.R., T.O., and T.V.L. analyzed data; and N.S., I.K., O.G.T., Y.L., L.S., W.H.R., T.O., and T.V.L. wrote the paper.

Reviewers: L.F., University of Oxford; and J.K., Washington University in St. Louis, Washington, University Physicians.

1. S. L. Hauser, B. A. C. Cree, Treatment of multiple sclerosis: A review. *Am. J. Med.* **133**, 1380–1390.e2 (2020).
2. K. Bjornevik *et al.*, Longitudinal analysis reveals high prevalence of Epstein-Barr virus associated with multiple sclerosis. *Science* **375**, 296–301 (2022).
3. A. K. Hedström *et al.*, High levels of Epstein-Barr virus nuclear antigen-1-specific antibodies and infectious mononucleosis act both independently and synergistically to increase multiple sclerosis risk. *Front. Neurol.* **10**, 1368 (2020), 10.3389/fneur.2019.01368.
4. M. Cortese *et al.*, Serologic response to the Epstein-Barr virus peptidome and the risk for multiple sclerosis. *JAMA Neurol.* **81**, 515–524 (2024).
5. A. K. Hedström, L. Alfredsson, T. Olsson, Environmental factors and their interactions with risk genotypes in MS susceptibility. *Curr. Opin. Neurol.* **29**, 293–298 (2016).
6. L. Moutsianas *et al.*, Class II HLA interactions modulate genetic risk for multiple sclerosis. *Nat. Genet.* **47**, 1107–1113 (2015).
7. T. Olsson, L. F. Barcellos, L. Alfredsson, Interactions between genetic, lifestyle and environmental risk factors for multiple sclerosis. *Nat. Rev. Neurol.* **13**, 25–36 (2017).
8. M. P. Pender, P. A. Csurhes, J. M. Burrows, S. R. Burrows, Defective T-cell control of Epstein-Barr virus infection in multiple sclerosis. *Clin. Transl. Immunology* **6**, e126 (2017).
9. O. G. Thomas, A. Rickinson, U. Palendira, Epstein-Barr virus and multiple sclerosis: Moving from questions of association to questions of mechanism. *Clin. Transl. Immunology* **12**, e1451 (2023).
10. A. Gottlieb, H. P. T. Pham, J. G. Saltarrelli, J. W. Lindsey, Expanded T lymphocytes in the cerebrospinal fluid of multiple sclerosis patients are specific for Epstein-Barr-virus-infected B cells. *Proc. Natl. Acad. Sci. U.S.A.* **121**, e2315857121 (2024).
11. T. Schneider-Hohendorf *et al.*, Broader Epstein–Barr virus-specific T cell receptor repertoire in patients with multiple sclerosis. *J. Exp. Med.* **219**, e20220650 (2022).
12. S. S. Soldan *et al.*, Multiple sclerosis patient-derived spontaneous B cells have distinct EBV and host gene expression profiles in active disease. *Nat. Microbiol.* **9**, 1540–1554 (2024).
13. J. B. Harley *et al.*, Transcription factors operate across disease loci, with EBNA2 implicated in autoimmunity. *Nat. Genet.* **50**, 699–707 (2018).
14. T. V. Lanz *et al.*, Clonally expanded B cells in multiple sclerosis bind EBV EBNA1 and GlialCAM. *Nature* **603**, 321–327 (2022).
15. N. R. Jog *et al.*, Epstein Barr virus nuclear antigen 1 (EBNA-1) peptides recognized by adult multiple sclerosis patient sera induce neurologic symptoms in a murine model. *J. Autoimmun.* **106**, 102332 (2020).
16. O. G. Thomas *et al.*, Cross-reactive EBNA1 immunity targets alpha-crystallin B and is associated with multiple sclerosis. *Sci. Adv.* **9**, eadg3032 (2023).
17. K. Tengvall *et al.*, Molecular mimicry between Anoctamin 2 and Epstein-Barr virus nuclear antigen 1 associates with multiple sclerosis risk. *Proc. Natl. Acad. Sci. U.S.A.* **116**, 16955–16960 (2019).
18. K. Ruprecht *et al.*, Multiple sclerosis: The elevated antibody response to Epstein-Barr virus primarily targets, but is not confined to, the glycine-alanine repeat of Epstein-Barr nuclear antigen-1. *J. Neuroimmunol.* **272**, 56–61 (2014).
19. N. Jafari *et al.*, No evidence for intrathecal IgG synthesis to Epstein Barr virus nuclear antigen-1 in multiple sclerosis. *J. Clin. Virol.* **49**, 26–31 (2010).
20. J. Salzer *et al.*, Epstein–Barr virus antibodies and vitamin D in prospective multiple sclerosis biobank samples. *Mult. Scler.* **19**, 1587–1591 (2013).
21. E. Sundqvist *et al.*, Epstein-Barr virus and multiple sclerosis: Interaction with HLA. *Genes Immun.* **13**, 14–20 (2012).
22. P. V. Lehmann, T. Forsthuber, A. Miller, E. E. Sercarz, Spreading of T-cell autoimmunity to cryptic determinants of an autoantigen. *Nature* **358**, 155–157 (1992).
23. Y. D. Dai, G. Carayanniotis, E. Sercarz, Antigen processing by autoreactive B cells promotes determinant spreading. *Cell. Mol. Immunol.* **2**, 169–175 (2005).
24. R. Martin, M. Sospedra, T. Eiermann, T. Olsson, Multiple sclerosis: Doubling down on MHC. *Trends Genet.* **37**, 784–797 (2021).
25. H. Zdimerova *et al.*, Attenuated immune control of Epstein-Barr virus in humanized mice is associated with the multiple sclerosis risk factor HLA-DR15. *Eur. J. Immunol.* **51**, 64–75 (2021).
26. N. Drosu *et al.*, CD4 T cells restricted to DRB1*15:01 recognize two Epstein–Barr virus glycoproteins capable of intracellular antigen presentation. *Proc. Natl. Acad. Sci. U.S.A.* **121**, e2416097121 (2024).
27. A. K. Hedström, M. Bäärnhielm, T. Olsson, L. Alfredsson, Tobacco smoking, but not Swedish snuff use, increases the risk of multiple sclerosis. *Neurology* **73**, 696–701 (2009).
28. International Multiple Sclerosis Genetics Consortium, Multiple sclerosis genomic map implicates peripheral immune cells and microglia in susceptibility. *Science* **365**, eaav7188 (2019).
29. H. Vietzen *et al.*, Ineffective control of Epstein–Barr-virus-induced autoimmunity increases the risk for multiple sclerosis. *Cell* **186**, 5705–5718.e13 (2023).
30. H. Vietzen *et al.*, Accumulation of Epstein-Barr virus-induced cross-reactive immune responses is associated with multiple sclerosis. *J. Clin. Invest.* **134**, e184481 (2024).
31. D. Jons *et al.*, Seroreactivity against lytic, latent and possible cross-reactive EBV antigens appears on average 10 years before MS induced preclinical neuroaxonal damage. *J. Neurol. Neurosurg. Psychiatry* **95**, 325–332 (2024).
32. M. De Paschale, P. Clerici, Serological diagnosis of Epstein-Barr virus infection: Problems and solutions. *World J. Virol.* **1**, 31–43 (2012).
33. W. Henle *et al.*, Antibody responses to Epstein-Barr virus-determined nuclear antigen (EBNA)-1 and EBNA-2 in acute and chronic Epstein-Barr virus infection. *Proc. Natl. Acad. Sci. U.S.A.* **84**, 570–574 (1987).
34. M.-S. Kang, E. Kieff, Epstein-Barr virus latent genes. *Exp. Mol. Med.* **47**, e131 (2015).
35. J. Dheekollu *et al.*, Cell-cycle-dependent EBNA1-DNA crosslinking promotes replication termination at oriP and viral episome maintenance. *Cell* **184**, 643–654.e13 (2021).
36. E. A. Leadbetter *et al.*, Chromatin-IgG complexes activate B cells by dual engagement of IgM and Toll-like receptors. *Nature* **416**, 603–607 (2002).
37. V. Laurynenka, L. Ding, K. M. Kaufman, J. A. James, J. B. Harley, A high prevalence of anti–EBNA1 heteroantibodies in systemic lupus erythematosus (SLE) supports anti–EBNA1 as an origin for SLE autoantibodies. *Front. Immunol.* **13**, 830993 (2022).
38. J. Huang *et al.*, Genetics of immune response to Epstein–Barr virus: Prospects for multiple sclerosis pathogenesis. *Brain* **147**, 3573–3582 (2024).
39. V. I. Zarnitsyna *et al.*, Masking of antigenic epitopes by antibodies shapes the humoral immune response to influenza. *Philos. Trans. R. Soc. Lond. B Biol. Sci.* **370**, 20140248 (2015).
40. S. S. Ousman *et al.*, Protective and therapeutic role for alphaB-crystallin in autoimmune demyelination. *Nature* **448**, 474–479 (2007).
41. E. Jeworutzki *et al.*, GlialCAM, a protein defective in a leukodystrophy, serves as a ClC-2 Cl(-) channel auxiliary subunit. *Neuron* **73**, 951–961 (2012).
42. H. Tamaki, B. L. Beaulieu, M. Somasundaran, J. L. Sullivan, Major histocompatibility complex class I–restricted cytotoxic T lymphocyte responses to Epstein–Barr virus in children. *J. Infect. Dis.* **172**, 739–746 (1995).
43. K. W. Wucherpfennig, J. L. Strominger, Molecular mimicry in T cell–mediated autoimmunity: Viral peptides activate human T cell clones specific for myelin basic protein. *Cell* **80**, 695–705 (1995).
44. K. Ota *et al.*, T-cell recognition of an immunodominant myelin basic protein epitope in multiple sclerosis. *Nature* **346**, 183–187 (1990).
45. P. Sundström, M. Nyström, K. Ruuth, E. Lundgren, Antibodies to specific EBNA-1 domains and HLA DRB1$_*$1501 interact as risk factors for multiple sclerosis. *J. Neuroimmunol.* **215**, 102–107 (2009).
46. E. Sundqvist *et al.*, Lack of replication of interaction between EBNA1 IgG and smoking in risk for multiple sclerosis. *Neurology* **79**, 1363–1368 (2012).
47. A. Manouchehrinia *et al.*, Plasma neurofilament light levels are associated with risk of disability in multiple sclerosis. *Neurology* **94**, e2457–e2467 (2020).
48. B. Ayoglu *et al.*, Anoctamin 2 identified as an autoimmune target in multiple sclerosis. *Proc. Natl. Acad. Sci. U. S. A.* **113**, 2188–2193 (2016).
49. C. R. Zamecnik *et al.*, An autoantibody signature predictive for multiple sclerosis. *Nat. Med.* **30**, 1300–1308 (2024).
50. A. D. Bandaranayake *et al.*, Daedalus: A robust, turnkey platform for rapid production of decigram quantities of active recombinant proteins in human cell lines using novel lentiviral vectors. *Nucleic Acids Res.* **39**, e143 (2011).
51. M. Bronge *et al.*, Identification of four novel T cell autoantigens and personal autoreactive profiles in multiple sclerosis. *Sci. Adv.* **8**, *eabn1823* (2022).
52. I. S. Kockum, Antibody levels towards Epstein Barr virus antigens and molecular mimics in multiple sclerosis patients and controls (Version 1) [Data set]. Swedish National Data Service. https://doi.org/10.48723/0xhc-vp63. Accessed 12 February 2025.